

# Structural–dynamical relationship in silica PEG hybrid gels

Philippe Lesot,<sup>a</sup> Séverin Chapuis,<sup>a</sup> Jean Pierre Bayle,<sup>a</sup> Jacques Rault,<sup>b</sup> Eric Lafontaine,<sup>c</sup> Antonio Campero<sup>d</sup> and Patrick Judeinstein<sup>\*a</sup>

<sup>a</sup>Laboratoire de Chimie Structurale Organique (URA CNRS 1384), Bât 410, Université Paris-Sud, 91405 Orsay, France

<sup>b</sup>Laboratoire de Physique des Solides, Bât 510, Université Paris-Sud, 91405 Orsay, France

<sup>c</sup>DGA/CREA, 16 bis Avenue Prieur de la Côte d'Or, 91144 Arcueil Cedex, France

<sup>d</sup>Departamento de Química, Universidad Autónoma Metropolitana Itzapalapa, 09340 Mexico D.F., Mexico

Hybrid organic–inorganic materials have been prepared from mixtures of tetraethoxysilane and poly(ethylene glycol) (PEG) of low molecular mass. These materials are diphasic systems in which silica aggregates, controlling the mechanical properties, are wrapped around by the polymer phase. Strong correlations between the synthesis scheme, the structure and the properties of these materials are evidenced. Solid-state <sup>29</sup>Si NMR points out the change of the silica morphology with the nature of the catalyst (acidic, [HCl] or nucleophilic, [NH<sub>4</sub>F]). In addition, these changes induce strong variations of the thermal properties of the PEG phase. The structural and dynamical inhomogeneities of the PEG are analyzed using <sup>13</sup>C NMR and EPR spectroscopies. Near the SiO<sub>2</sub> surfaces, hydrogen bonding hinders the motion of the PEG chains, while the bulk of the polymeric phase possesses the same properties as the polymer melt. Thermal analyses (DSC) disclose the difference between materials prepared with the various catalysts which are related to the degree of interpenetration between the two phases.

The design and synthesis of organic–inorganic nanocomposites is a fascinating area with numerous scientific and technological interests in the fields of optics, mechanics, ionoelectronics and biology.<sup>1</sup> These materials, termed 'hybrids', are diphasic media in which both inorganic and organic phases play major roles in the chemical and physical properties. Nevertheless, it is inadequate to take into account their individual contributions in order to completely explain the properties of these blends. Consequently, the synergy between the two phases can only be explained by the effects of the size of the domains and the properties of the interfaces.<sup>2</sup> Thus, these materials were recently discriminated into two distinct classes with respect to the chemical nature of the organic–inorganic interface. In materials of class I, organic and inorganic components are mixed together and only ionic or weak bonds (hydrogen, van der Waals...) govern the cohesion of the whole structure. In materials of class II, the two phases are linked together through strong chemical bonds (covalent or ionocovalent bonds).<sup>3</sup>

Nanocomposites obtained from silica (SiO<sub>2</sub>) and poly(ethylene glycol) (PEG) have already been described.<sup>4</sup> The silica network forms a 'solid-like' matrix wrapped around by the polymer phase. Thus, these materials can be considered as a 'solid solvent' in which various entities such as molecules, macromolecules or salts can be easily dissolved.<sup>5,6</sup>

At present, the sol–gel process appears to be the unique way of designing such materials. Starting from molecular precursors, we can obtain a solid matrix with a controlled porosity. The mixing of organic and inorganic moieties at the molecular level leads to materials with totally new properties. The choice of the reaction parameters (solvent, catalyst, precursor...) is an essential point to control both the growth and the morphology of the aggregates and is also a key point to finely tune their final properties.<sup>7</sup>

This paper reports the study of silica/poly(ethylene glycol) materials of class I synthesised under different catalysis conditions, acidic (HCl) or nucleophilic (NH<sub>4</sub>F) and for a wide range of chemical compositions. The structure of the silica clusters inside these blends was investigated by solid-state <sup>29</sup>Si NMR spectroscopy. The nature of the PEG phase is

investigated by liquid-state <sup>13</sup>C NMR measurements, EPR spectroscopy using stable nitroxide radicals dissolved in the polymer phase and DSC. All these analytical techniques were used to probe the molecular motion inside the PEG phase. They unambiguously proved that the polymer component exhibits a strong dynamical heterogeneity. Moreover, the relationship between the morphology of the silica clusters and the dynamical properties of the PEG, which are mainly governed by the silica/polymer interface and the size of the domains, has also been explored.

## Results

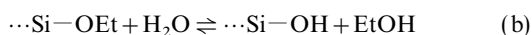
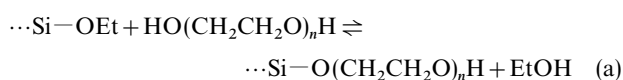
### Synthesis

All chemical reagents were commercially available. These include tetraethoxysilane (TEOS) as silica precursor, diethylene glycol (PEG<sub>106</sub>) and poly(ethylene glycol) [PEG<sub>*n*</sub>, where *n* is the molecular mass (*n* = 200 or 300)] as organic macromers, hydrochloric acid (HCl) and ammonium fluoride (NH<sub>4</sub>F) as catalysts, and amino-TEMPO (4-amino-2,2,6,6-tetramethylpiperidin-1-oxyl) as a stable radical for the EPR investigations. Deionized water was used in all experiments.

For the sake of clarity, the A[*x*]<sub>*n*</sub> nomenclature was applied for the materials described in this work. A represents the type of catalyst, H or N respectively for an acidic (HCl) or nucleophilic (NH<sub>4</sub>F) catalyst, *x* is the fraction (in mass%) of silica inside the final hybrid (considering that all ethoxy groups are removed after hydrolysis–condensation) and *n* is the average molecular mass of the PEG. For all materials, the catalyst ratio ([catalyst]/[Si]) was kept constant and equal to 10<sup>−3</sup>. For the different investigated series, the silica fractions, *x*, are 4.7, 13, 23, 37, 54 and 60 mass%. Finally, the hydrolysis ratio ([H<sub>2</sub>O]/[Si]) was set to 10.

The synthesis of a representative H[23]<sub>200</sub> material is described below: TEOS (1 g, 4.8 × 10<sup>−3</sup> mol) was added to PEG<sub>200</sub> (0.97 g, 4.8 × 10<sup>−3</sup> mol) and 0.86 g of an aqueous catalyst solution (4.8 × 10<sup>−2</sup> mol H<sub>2</sub>O + 4.8 × 10<sup>−6</sup> mol HCl) under vigorous stirring. EtOH (1 ml) was then added and the mixture was heated to 60 °C and stirred for 10 min. The liquid

mixture was cast in an open-air PTFE vessel at room temperature for 2 days, then aged during 5 days at 80 °C before drying under vacuum (48 h, 10<sup>-2</sup> mm Hg, 80 °C) in order to entirely evaporate the solvents. This last process was monitored by IR spectroscopy. Transparent monolithic materials were obtained for acidic catalysis whereas white powders were obtained when NH<sub>4</sub>F was used as catalyst. The formation and structure of SiO<sub>2</sub>/PEG materials of class I obtained under similar conditions have been described elsewhere.<sup>6</sup> Under acidic catalysis, the fast kinetics of hydroxylation and condensation of TEOS lead to the rapid formation of silica clusters and transparent monoliths are finally obtained. The gelation time of such systems is *ca.* 100 h. In contrast, when neutral catalysis is used, the white powdery gels are formed within a few minutes after mixing of the reactants. Note that the transesterification reaction between TEOS and PEG (a) competes with hydroxylation (b). This equilibrium, (b), is then followed by condensation step (c) thus leading to the formation of a silica network itself. However, reactions (b) and (c) are predominant over (a), and the ratio of PEG bonded to silicon in the final material is <10% of the available sites.



### Solid-state <sup>29</sup>Si NMR spectroscopy

Solid-state NMR spectra were recorded on a Bruker MSL-200 spectrometer at 39.73 MHz for <sup>29</sup>Si. The samples were filled in fused zirconia rotor fitted with Kel-F caps and spun at 4 kHz at the magic angle (54.7°). <sup>29</sup>Si chemical shifts were referenced relative to TMS (δ0) used as the external reference. CP MAS NMR spectra were obtained using a cross-polarization sequence and broadband high power decoupling during acquisition. For these experiments, the NMR parameters were a 20 s recycle delay, a 5 ms mixing time and a 4.1 μs proton 90° pulse. This technique enhances the magnetization of the rare <sup>29</sup>Si spin from that of the abundant <sup>1</sup>H spins of the polymer and principally silicon atoms near the interface are probed by this technique. High power (HP) decoupling MAS NMR spectra were recorded using permanent broad band high power <sup>1</sup>H decoupling with a recycle delays of 60 s. The 90° silicium pulses were of 6 μs duration. The low spatial selectivity of the high power (HP) radio frequency decoupling allows visualisation of the whole structure of the silica aggregates.

Fig. 1 shows the <sup>29</sup>Si MAS NMR spectra of materials H[13]<sub>200</sub> and N[13]<sub>200</sub> obtained using the CP and HP decoupling modes. In both spectra, two wide signals centred around δ -101 and -111 are observed. These signals are characteristic of Q<sup>3</sup> [XOSi\*(OSi)<sub>3</sub>, X=H or C] and Q<sup>4</sup> [Si\*(OSi)<sub>4</sub>] environments.<sup>8</sup> The absence of Q<sup>2</sup> signals [XO<sub>2</sub>Si\*(OSi)<sub>2</sub>] confirms the strong development of the silica condensation inside both of these blends. The signals were deconvoluted with two Lorentzian shaped signals and the results of the data treatments are summarized in Table 1.

**Table 1** Deconvolution parameters of the different signals obtained by <sup>29</sup>Si{<sup>1</sup>H} NMR spectroscopy

| TEOS catalyst     | decoupling mode | ratio area Q <sup>3</sup> /area Q <sup>4</sup> | Q <sup>3</sup> linewidth /Hz | Q <sup>4</sup> linewidth /Hz |
|-------------------|-----------------|--|------------------------------|------------------------------|
| HCl               | HP-DEC          | 1.5  | 170                          | 270                          |
| HCl               | CP              | 3.0  | 170                          | 290                          |
| NH <sub>4</sub> F | HP-DEC          | 0.7  | 930                          | 520                          |
| NH <sub>4</sub> F | CP              | 1.0  | 500                          | 600                          |

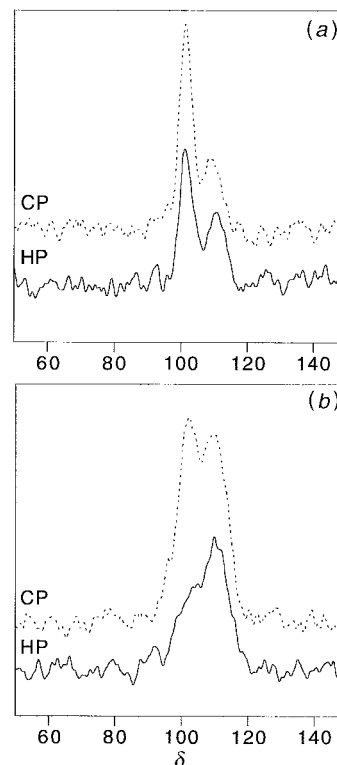


**Fig. 1** <sup>29</sup>Si MAS NMR spectra of (a) H[13]<sub>200</sub>, (b) N[13]<sub>200</sub> samples obtained in CP and HP decoupling modes

In both samples, the ratio Q<sup>3</sup>/Q<sup>4</sup> is larger for CP decoupled experiments than for HP decoupling conditions. The silicon atoms at the silica-polymer surface are enhanced by the CP technique compared to those of the core of the SiO<sub>2</sub> aggregates.<sup>9</sup> High power (HP) radiofrequency decoupling enables a better visualization of the complete structure of the silica aggregates.

Larger Q<sup>3</sup>/Q<sup>4</sup> ratios and important differences between HP and CP decoupling modes were measured for the acidic catalyzed materials, probing the large specific surface of these aggregates. It shows the lower degree of condensation of the silicon atoms inside these materials and the corresponding aggregates of silica can be described in terms of branched and polymeric morphologies. Conversely, more numerous Q<sup>4</sup> sites and broader signals were observed with nucleophilic catalyzed materials. This is related to the more compact structure of these silica aggregates. The width of the signal corresponds to more disordered local structure of the silicon atoms in the silica matrix as confirmed by recent X-ray diffraction measurements.<sup>10</sup>

### <sup>13</sup>C liquid-state NMR spectroscopy

Liquid-state <sup>13</sup>C NMR experiments were performed on an AM250 Bruker spectrometer (<sup>13</sup>C frequency 62.9 MHz) at room temperature on static samples. Proton broad-band decoupling was used to eliminate the residual <sup>1</sup>H-<sup>13</sup>C dipolar couplings. The finely ground powders were poured in 10 mm NMR tubes and <sup>13</sup>C{<sup>1</sup>H} spectra were obtained without deuterium lock control. Peak areas were measured following standard procedures and the calibration of the signal intensity was performed before each measurement with a sample of pure PEG<sub>200</sub>.

NMR spectroscopy provides an useful and attractive approach to describe the structure and the dynamics of the organic phase in hybrid materials. In complex systems, the heterogeneous character of the polymer phase can be investigated by a specific NMR approach in using selective techniques to discriminate the 'solid-like' and the 'liquid-like' parts. The use of 'liquid-like' conditions to record the spectra (static samples, broad-band decoupling using a moderate power) acts as a spectroscopic filter thus allowing observation of only the

mobile molecules. The percentage of 'liquid-like' molecules is then deduced from the ratio of the measured signal surface to the calculated one if all  $^{13}\text{C}$  nuclei were observable.<sup>11</sup>

The  $^{13}\text{C}\{^1\text{H}\}$  spectra of these materials present two broad bands centred around  $\delta$  60 and 69 (linewidth *ca.* 100 Hz) and corresponding to terminal and central ethylene groups, respectively, of the 'liquid-like' PEG molecules. Fig. 2 shows the evolution of the 'liquid-like' fraction with  $\text{SiO}_2$  content for materials of series  $\text{H}[x]_n$  and  $\text{N}[x]_n$  ( $n=106, 200, 300$ ). These evolutions clearly indicate the increase of a 'solid-like' phase as a function of the mass% of silica and are more pronounced for materials synthesized under acidic catalysis than for materials prepared under nucleophilic conditions.

### EPR spectroscopy

The EPR spectra were recorded at room temperature on an ER200 Bruker spectrometer operating at a frequency of 9.7 GHz. The microwave power level (20 mW), the modulation ( $5 \times 10^{-2}$  G) and the time constant (0.05 s) were carefully set to obtain a narrow linewidth. Amino-TEMPO radical was added to the reaction mixture as an EPR probe. This is an accurate method to determine the dynamics of molecular tumbling. However, EPR experiments could be only performed for nucleophilic catalyzed materials owing to strong degradation of the nitroxide groups in acidic media. Fig. 3 shows EPR spectra of the  $\text{N}[4.7]_{300}$ ,  $\text{N}[35]_{300}$  and  $\text{N}[60]_{300}$  compounds. The spectral shape is complex and cannot be fitted by a single line.<sup>12</sup> Best fits are achieved when using a superposition of broad and narrow components. This approach has already been applied to characterize polymers at solid interfaces,<sup>13</sup> interpenetrated networks<sup>14</sup> or nanocomposites of class II PEO/ $\text{SiO}_2$ .<sup>15</sup> The narrow component corresponds to the sharp spectrum of the initial solution (correlation time,  $\tau_R \approx 10^{-10}$  s), while the broad one is due to the corresponding frozen solution ( $\tau_R \approx 10^{-7}$  s). Because nitroxide probes are selectively dissolved in the organic phase, these results evidence the diphasic character of the PEG phase. The percentage of

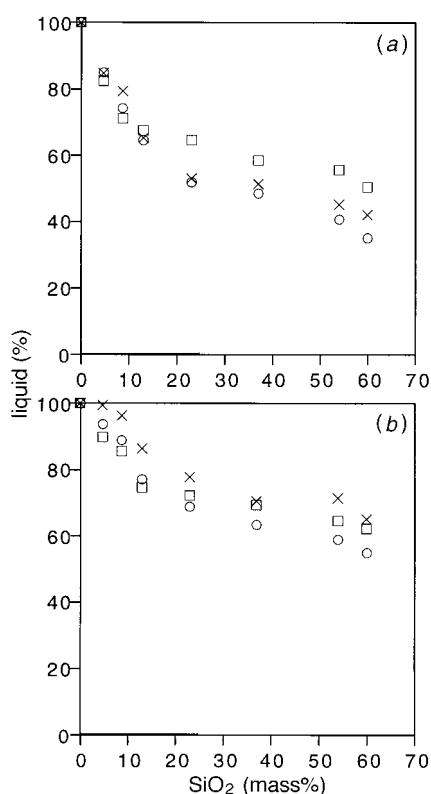


**Fig. 2** Evolution of the liquid-like ratio with the silica content for (a)  $\text{H}[x]_n$  and (b)  $\text{N}[x]_n$  series [ $n=106$  ( $\circ$ ), 200 ( $\square$ ), 300 ( $\times$ )], as determined from  $^{13}\text{C}\{^1\text{H}\}$  liquid-state NMR spectra

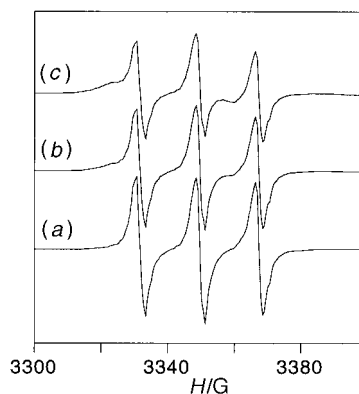


**Fig. 3** EPR spectrum of (a)  $\text{N}[4.7]_{200}$ , (b)  $\text{N}[35]_{200}$  and (c)  $\text{N}[60]_{200}$  compounds doped with nitroxide compounds

'liquid-like' region is 95, 85 and 70% in materials containing 4.7, 35 and 60% silica, respectively. Fig. 4 shows the variation of the 'liquid-like' PEG ratio with the silica content for the three series. A gradual decrease of the liquid component is observed upon increasing the silica content.

### DSC analyses

Differential scanning calorimetry (DSC) measurements were performed on a DSC30 Mettler microcalorimeter. Samples were cooled to  $-120^\circ\text{C}$  and measurements were performed by heating to  $90^\circ\text{C}$  (rate  $10^\circ\text{C min}^{-1}$ ) for two runs. The temperatures  $T_g$  were determined from the midpoint of the experimental curves. The DSC curves of the  $\text{H}[x]_{300}$  and  $\text{N}[x]_{300}$  series ( $x=5.4, 23, 37$  and  $54$ ) are shown in Fig. 5(a) and (b). These characteristic curves are reproducible even after a first scan up to  $150^\circ\text{C}$ .

The thermal behavior of  $\text{H}[x]_{300}$  and  $\text{N}[x]_{300}$  series is totally different. For acidic series, the different samples present only a glass transition  $T_g$ . The temperature  $T_g$  increases with inorganic content rising from  $-82^\circ\text{C}$  for the sample containing 5.4 mass% silica to  $-40^\circ\text{C}$  when silica content is 60 mass%. This variation is continuous, and conversely, the width of the glass transition step increases. The different series  $\text{H}[x]_n$  show the same behavior and  $T_g$  values are plotted in Fig. 6(a). For a defined silica ratio,  $T_g$  increases with the PEG molecular mass, following the behavior of the pure organic compound.

The properties of materials  $\text{N}[x]_{300}$  obtained under nucleophilic conditions are totally different [Fig. 5(b)]. With the exception of the compound with the highest silica content, all these materials show similar DSC curves with a glass transition ( $T_g$ ) at  $-82^\circ\text{C}$ , a cold crystallization ( $T_c$ ) around  $-60^\circ\text{C}$  associated with a melting peak ( $T_m$ ) around  $-18^\circ\text{C}$ . These transitions are also similar to those of the pure  $\text{PEG}_{300}$ . The

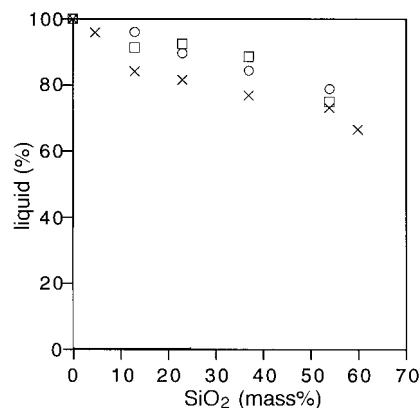


**Fig. 4** Evolution of the liquid-like ratio with silica content for  $n=106$  ( $\circ$ ), 200 ( $\square$ ), 300 ( $\times$ ), from EPR spectra

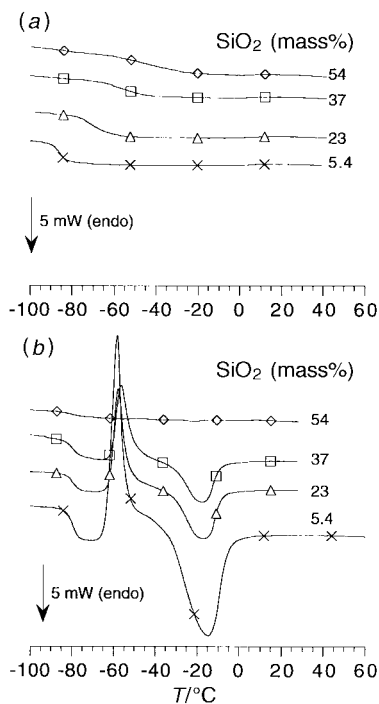


Fig. 5 Experimental DSC curves of compounds of (a)  $H[x]_{200}$  and (b)  $N[x]_{200}$  series

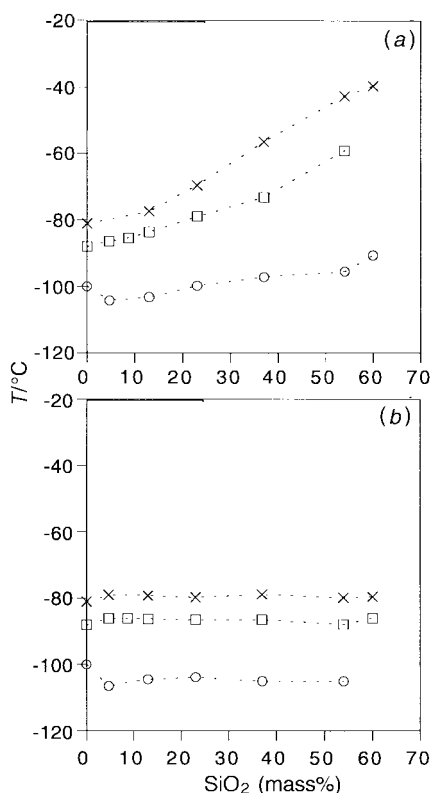


Fig. 6 Evolution of the transition temperature for series (a)  $N[x]_n$  and (b)  $H[x]_n$  [ $n=106$  (○), 200 (□), 300 (×)]

material  $N[60]_{300}$  presents only a  $T_g$  which is also at  $-82^\circ\text{C}$ . Over the entire composition range, the different series  $N[x]_n$  present similar behavior, with  $T_g$  temperatures identical to the pure  $PEG_n$  compounds.

## Discussion

PEG/silica nanocomposites of class I are easily synthesized by the sol-gel process at room temperature by using different

catalysts such as hydrochloric acid (HCl) or ammonium fluoride ( $\text{NH}_4\text{F}$ ). Transparent monolithic materials are obtained only after a few days under acidic catalysis, whereas nucleophilic conditions give white powders in a few hours. Obviously, these observations reflect the difference in the reaction steps which are involved during the building of the architecture of the silica clusters.

$^{29}\text{Si}$  solid-state NMR spectra are very sensitive to the structure of the silica.<sup>16</sup> A lower degree of condensation is observed in materials prepared by acidic catalysis and corresponds to silica clusters which are weakly branched polymers with bushy shapes. These structures are characteristic of materials with a large ratio of silicon atoms at the interface within the polymer and correspond to a high surface interface with the organic component. In contrast, the materials prepared under nucleophilic conditions show a higher degree of condensation which characterizes more compact and denser silica particles. Consequently, for materials with similar compositions, a smaller interface between both components is seen in the nucleophilic catalysed materials.

Such changes in the morphology of the silica network with the conditions of the reactions were also observed when silica was obtained from hydrolysis of silicon alkoxides in dilute solutions and correspond to the relative rates of the hydrolysis and condensation steps.<sup>17</sup> In these nanocomposites, changes of the degree of interpenetration between both phases are expected with modification of the cluster morphologies.<sup>18</sup> Furthermore, the chemical nature of the interface itself (ratio of hydroxyl, ethoxy and PEG bonded) should be also different.<sup>19</sup>

The study of the dynamics inside the PEG phase characterizes the nature of this interfacial zone.<sup>20</sup> Liquid-state  $^{13}\text{C}$  NMR, EPR of dissolved nitroxide probes and thermal analysis (DSC) evidence the heterogeneity of the polymeric phase owing to the simultaneous presence of 'liquid-like' and 'solid-like' phases.

First, only 'liquid-like' PEG molecules are observed by liquid-state  $^{13}\text{C}$  NMR and EPR spectroscopy when nitroxide molecules are dissolved inside the material. The linewidth of the signals and preliminary  $T_1$  and  $T_2$  measurements indicate that the viscosity of the 'liquid-like' PEG phase inside nanocomposites is much higher than the pure melt of corresponding PEG chains.<sup>21</sup> The characteristic NMR correlation time,  $\tau_c$ , is expected to be in the range of  $10^{-7}$ – $10^{-9}$  s,<sup>22</sup> whereas the EPR correlation time  $\tau_R$  is in the range of  $10^{-10}$  s.<sup>13</sup> These two spectroscopies provide different information on the kind of molecules and motion modes in our medium. EPR measures the rotational diffusion of small molecules dissolved inside the polymeric phase while NMR gives some insight on the complex reorientational behavior of the polymer chains.<sup>23</sup> The hindrance of motion for the polymer segments is related to conformational and steric hampering inside the restricted geometries of the silica clusters.<sup>24</sup>

Secondly, 'solid-like' PEG molecules are characterized by slow dynamics ( $\tau_c < 10^{-7}$  s).<sup>22</sup> As a consequence, they cannot be observed by the NMR measurement conditions described here. Nevertheless, our liquid-state NMR experiments could be easily used to estimate the 'liquid-to-solid' ratio as a function of the disappearing signal. In a previous study,  $^{29}\text{Si}$ - $^1\text{H}$  correlation NMR spectroscopy was reported on similar acid catalyzed materials.<sup>6</sup> This work demonstrated conclusively that the 'solid-like' PEG component corresponds to molecules which are located at the surface of the silica clusters. Clearly, the reactivity of the silica surface enables the formation of chemical bonds with the PEG molecules and also weaker hydrogen bonds between the silanol groups and the ether oxygen of the PEG molecules. Then, the mobility of the few polymer layers covering the oxide clusters is strongly hindered, as reported for layers of polymer deposited on silicon wafers or porous silica glass.<sup>13,20b</sup>

The experimental data (EPR, NMR and DSC) show unambiguously the heterogeneous character of the polymer phase.

The EPR spectra show the presence of two components indicating a bimodal distribution of the motion modes of the PEG molecules. These measurements also demonstrate the strong increase of the 'solid-like' character of the PEG at the expense of the 'liquid-like' component when the ratio of silica to polymer increases. This can be related to the increase of the growth of the silica surface by increasing the inorganic character of these materials. However, the effects of the catalytic system and the PEG chain length are more complicated and are probably beyond the scope of these measurements.

Finally, DSC measurements give further information on the influence of the silica structure on the polymer properties. In the series prepared under nucleophilic conditions, the behavior of the PEG phase is not influenced by the silica while the PEG phase is strongly disturbed by the proximity of the oxide phase in materials prepared under acidic conditions.

These thermal measurements show that acid catalysis leads to homogeneous blends in which the glass transition temperature of the PEG is shifted and broadened by the proximity of the silica. These effects are due to the increase in rigidity of the PEG chains when the number and the strength of the Si—polymer bonds increase. Most of these links are certainly hydrogen bonds even if some Si—O—polymer bonds were previously indicated by NMR measurement.<sup>6</sup> PEG chains can be considered as co-monomers of the silica which prevents cold crystallization of the organic phase.<sup>25</sup> The broadening of the glass transition with increase in silica content indicates a large distribution of the confinement distance of the PEG inside the silica structure. This behavior is similar to that in cross-linked polymers when there is a large distribution of distances between cross-links.<sup>25,26</sup> These effects emphasize the strong confinement of the organic and inorganic phases.

For materials prepared under nucleophilic conditions, the PEG phase is not influenced by the silica. This means that even at a high silica ratio, the PEG phase has only weak interaction with the silica surface. This could be a consequence of the lower specific surface of the oxide.

## Conclusion

This work presents a detailed study of class I silica-PEG hybrid materials. These nanocomposites obtained by the condensation of silica inside low molecular mass PEG have complex structures which are strongly dependent on the synthesis conditions. Their architectures were investigated by either looking at the silica networks by <sup>29</sup>Si NMR spectroscopy, or at the polymer phase by liquid-state <sup>13</sup>C NMR, EPR and thermal analyses. These studies demonstrate the interpenetration between organic and inorganic phases and the strong influence of the interface on the final properties. Further experimental studies are under way to depict the effect of the synthesis on the structure and properties of these compounds. This might provide new information capable of enhancing our knowledge of the interfacial zone.

## References

- 1 See, for example: (a) *Better Ceramics Through Chemistry VI*, ed. A. K. Cheetham, C. J. Brinker and M. L. McCartney, *Mater. Res. Soc. Symp. Proc.*, 1994, **346**; (b) *Better Ceramics Through Chemistry VII*, ed. A. K. Cheetham, C. J. Brinker and M. L. McCartney, *Mater. Res. Soc. Symp. Proc.*, 1996, **435**; (c) *Hybrid Organic-Inorganic Materials*, ed. C. Sanchez and F. Ribot, *New J. Chem.*, 1994, **18**; (d) *Hybrid Organic-Inorganic Composites*, ed. J. E. Mark, C. Y.-C. Lee and P. A. Bianconi, *ACS Symp. Ser.*, 1995, **585**.
- 2 (a) C. Sanchez and F. Ribot, *New J. Chem.*, 1994, **18**, 1007; (b) P. Judeinstein and C. Sanchez, *J. Mater. Chem.*, 1996, **6**, 511.
- 3 (a) B. M. Novak, *Adv. Mater.*, 1993, **5**, 422; (b) C. Sanchez and F. Ribot, *New J. Chem.*, 1994, **18**, 1007.
- 4 (a) D. Ravaine, A. Seminel, Y. Charbouillot and M. Vincens, *J. Non-Cryst. Solids*, 1986, **82**, 210; (b) S. Kohjiya, K. Ochiai and S. Yamashita, *Polymer Gels*, ed. D. DeRossi, Plenum Press, New York, 1991, p. 77; (c) D. E. Rodriguez, A. B. Brennan, C. Betrabet, B. Wang and G. L. Wilkes, *Chem. Mater.*, 1992, **4**, 1437.
- 5 P. Judeinstein and H. Schmidt, *J. Sol-Gel Sci. Technol.*, 1994, **3**, 189.
- 6 P. Judeinstein, J. Titman, M. Stamm and H. Schmidt, *Chem. Mater.*, 1994, **6**, 127.
- 7 J. Livage, M. Henry and C. Sanchez, *Prog. Solid State Chem.*, 1988, **18**, 259.
- 8 (a) G. Engelhardt, *High-Resolution Solid-State NMR of Silica and Zeolites*, Wiley, New York, 1987, p. 76; (b) R. K. Harris and R. H. Newman, *J. Chem. Soc., Faraday Trans.*, 1977, **73**, 1204.
- 9 N. Zumbulyadis and J. M. O'Reilly, *Macromolecules*, 1991, **24**, 5294.
- 10 M. Laridjani, E. Lafontaine and P. Judeinstein, unpublished work.
- 11 P. Judeinstein, P. W. Oliveira, J. P. Bayle and J. Courtieu, *J. Chim. Phys.*, 1994, **91**, 1583.
- 12 EPRL software package developed by D. J. Schneider and J. H. Freed, *Biological Magnetic Resonance*, ed. L. J. Berliner and J. Reuben, Plenum, New York, 1989.
- 13 H. Hommel, *Adv. Colloid Interface Sci.*, 1995, **54**, 209.
- 14 T. Marinovic, S. Valic, M. Andreis and Z. Veksli, *Polymer*, 1994, **32**, 2519.
- 15 M. E. Brik, J. P. Bayle, J. Titman and P. Judeinstein, *J. Polym. Sci., Part B: Polym. Phys.*, 1996, **34**, 2533.
- 16 K. L. Walther, A. Wokaun and A. Baiker, *Mol. Phys.*, 1990, **71**, 769.
- 17 R. J. P. Corriu and D. Leclercq, *Angew. Chem., Int. Ed. Engl.*, 1996, **35**, 1421.
- 18 I. A. David and G. W. Scherer, *Chem. Mater.*, 1995, **7**, 1957.
- 19 D. W. Sindorf and G. E. Maciel, *J. Phys. Chem.*, 1982, **86**, 5208.
- 20 See, for example: (a) *Molecular Dynamics in Restricted Geometries*, ed. J. Klafter and J. M. Drake, Wiley, New York, 1989; (b) *Polymers at Interfaces*, ed. G. J. Fleer, M. A. Cohen Stuart, T. Cosgrove and B. Vincent, Chapman & Hall, London, 1993.
- 21 S. Xu and J.-P. Korb and J. Jonas, *Mater. Res. Soc. Symp. Proc.*, 1994, **346**, 925.
- 22 C. P. Grey and K. G. Sharp, *Mater. Res. Soc. Symp. Proc.*, 1996, **435**, 179.
- 23 U. M. Biermann, W. Mikosch, T. Dorfmueller and W. Eimer, *J. Phys. Chem.*, 1996, **100**, 1705.
- 24 S. Stapf and R. Kimmich, *Macromolecules*, 1996, **29**, 1638.
- 25 See, for example, H. Van Krevaleen, *Properties of Polymers*, Elsevier, Amsterdam, 1985.
- 26 E. W. Hansen, M. Stöcker and R. Schmidt, *J. Phys. Chem.*, 1996, **100**, 2195.

Paper 7/04983H; Received 11th July, 1997